Ring-Opening Polymerization Behavior of *ansa*- and Spirocyclic *ansa*-Zirconocene Complexes

Timothy J. Peckham,[†,⊥] Paul Nguyen,[‡,⊥] Sara C. Bourke,[⊥] Qinyan Wang,[§] Daryll G. Harrison,[§] Peter Zoricak,[§] Charles Russell,[§] Louise M. Liable-Sands,[∥] Arnold L. Rheingold,[∥] Alan J. Lough,[⊥] and Ian Manners*

Department of Chemistry, University of Toronto, 80 St. George Street, Toronto, Ontario, Canada M5S 3H6, Nova Chemicals, 2928-16 Street N.E., Calgary, Alberta, Canada T2E 7K7, and Department of Chemistry and Biochemistry, University of Delaware, Newark, Delaware 19716

Received November 30, 2000

Attempts to develop a ring-opening polymerization (ROP) approach to polymeric zirconocene complexes are reported. A new silicon-bridged [1][1]zirconocenophane, $(SiMe_2)_2(\eta^5\text{-}C_5H_3)_2Zr(NEt_2)_2$ (**3a**), was synthesized by reaction of $Zr(NEt_2)_4$ with $(C_5H_4)_2(SiMe_2)_2$ (**4**). Single-crystal X-ray diffraction revealed a highly tilted structure with an angle of 73.1(4)°, a significant increase over the untethered compound $(\eta^5\text{-}MeC_5H_4)_2ZrCl_2$ (**2**), which possesses a tilt angle of 54.2°. This and the related compounds $(SiMe_2)(\eta^5\text{-}C_5H_4)_2MCl_2$ (**1a**, M = Ti; **1b**, M = Zr) and $(SiMe_2)_2(\eta^5\text{-}C_5H_3)_2ZrCl_2$ (**3b**) were tested for transition-metal catalyzed ROP behavior in the presence of Pt(0) catalysts but were found to be inactive. The novel spirocyclic silacyclobutane-bridged monomer $(CH_2)_3Si(\eta^5\text{-}C_5H_4)_2ZrCl_2$ (**7b**) was prepared via a "fly trap" amine elimination reaction between cyclotrimethylenedicyclopentadienylsilane (**8**) and $Zr(NMe_2)_4$; this initially yielded $(CH_2)_3Si(\eta^5\text{-}C_5H_4)_2Zr(NMe_2)_2$ (**7a**), which was converted to **7b** by reaction with a slight excess of Me_3SiCl. **7a** and **7b** were characterized by ^{29}Si, ^{13}C, and ^1H NMR spectroscopy and mass spectrometry as well as single-crystal X-ray diffraction. Both showed moderate tilt angles (61.7(2)° and 59.69(7)°, respectively) as well as highly strained silacyclobutane rings with C−Si−C bond angles of 79.7(2)° and 80.64(10)°, respectively. Transition-metal-catalyzed ROP of **7b** led to the formation of the polycarbosilane $[(CH_2)_3Si(\eta^5\text{-}C_5H_4)_2ZrCl_2]_n$ (**10**). Both the soluble and insoluble fractions of **10** were characterized by CP-MAS ^{29}Si and ^{13}C NMR, and the soluble, oligomeric fraction was further characterized by solution ^{29}Si, ^{13}C, and ^1H NMR. Complexes **7a**, **7b**, and polyzirconocene **10** were found to exhibit moderate activity as ethylene polymerization catalysts.

Introduction

The synthesis and study of transition-metal-containing polymers is currently an active area of research, largely due to the possibility of combining the processibility commonly found in organic polymers with the many interesting aspects of transition metals, such as novel optical, electronic, electrical, and magnetic properties.[1] Of particular interest has been the inclusion of transition-metal moieties that are known to be catalytically active.

In the area of homogeneous Ziegler−Natta catalysis, the number of single-site metallocene-based catalyst systems has grown rapidly over the last twenty years along with an understanding of how to tailor such systems to achieve controlled stereoregularities.[2,3] However, heterogeneous catalysts offer the advantages of morphology control of the resultant polymer and a need for much lower activator-to-metallocene ratios.[4,5] A desire to combine the advantages of homogeneous and heterogeneous catalysts has provided a motivation for the synthesis of supported Ziegler−Natta catalysts such as single-site catalysts on insoluble inorganic substrates, including SiO_2 and MCM-41,[6] or attached to polymeric backbones, such as polysiloxanes and polystyrene.[7] Macromolecular supports have the potential advantage of being able to provide much more defined catalyst

* To whom all correspondence should be addressed. E-mail: imanners@chem.utoronto.ca. Fax: (416) 978-6157.
† Current address: Ballard Advanced Materials, 9000 Glenlyon Parkway, Burnaby, BC, Canada V5J 5J9.
‡ Current address: Bayer Inc., 1265 Vidal St. S., Sarnia, Ontario, Canada N7T 7M2.
⊥ University of Toronto.
§ Nova Chemicals.
∥ University of Delaware.

(1) (a) Manners, I. *Angew. Chem., Int. Ed. Engl.* **1996**, *35*, 1603−1621. (b) Gorman, C. *Adv. Mater.* **1998**, *10*, 295−309. (c) Puddephatt, R. J. *Chem. Commun.* **1998**, 1055−1062. (d) Hearshaw, M. A.; Moss, J. R. *Chem. Commun.* **1999**, 1−8. (e) Nguyen, P.; Gómez-Elipe, P.; Manners, I. *Chem. Rev.* **1999**, *99*, 1515−1548. (f) Pickup, P. G. *J. Mater. Chem.* **1999**, *9*, 1641−1653. (g) Kingsborough, R. P.; Swager, T. M. *Prog. Inorg. Chem.* **1999**, *48*, 123−231.

(2) Brintzinger, H. H.; Fischer, D.; Mülhaupt, R.; Rieger, B.; Waymouth, R. M. *Angew. Chem., Int. Ed. Engl.* **1995**, *34*, 1143−1170, and references therein.

(3) Herrmann, W. A.; Cornils, B. *Angew. Chem., Int. Ed. Engl.* **1997**, *36*, 1048−1067.

(4) Abbenhuis, H. C. L. *Angew. Chem., Int. Ed.* **1999**, *38*, 1058−1060.

(5) Alt, H. G. *J. Chem. Soc., Dalton Trans.* **1999**, 1703−1709.

(6) For recent examples see: (a) Lee, D.-H.; Yoon, K.-B.; Noh, S. K. *Polym. Prepr. (Am. Chem. Soc., Div. Polym. Chem.)* **1997**, *38*, 245−246. (b) Van Looveren, L. K.; Geysen, D. F.; Vercruysse, K. A.; Wouters, B. H.; Grobet, P. J.; Jacobs, P. A. *Angew. Chem., Int. Ed.* **1998**, *37*, 517−520. (c) Tudor, J.; O'Hare, D. *Chem. Commun.* **1997**, 603−604.

10.1021/om001023p CCC: $20.00
Publication on Web 06/08/2001

environments than inorganic solid supports. However, despite a significant amount of research in this area there are very few examples of well-characterized systems, and to date the rational design approaches that have made homogeneous catalysts themselves so successful have not been implemented.[8]

Extensive work performed in our research group has been based on the synthesis of polyferrocenes via the ring-opening polymerization (ROP) of strained ferrocenophanes (eq 1).[9] Thermal, anionic, and transition-metal ROP strategies have been shown to be effective with these systems.[9b] In this paper we report on our initial attempts to develop ROP approaches to supported group IV metallocene catalysts in which the catalytically active site is located in the polymer backbone itself or as a side group.

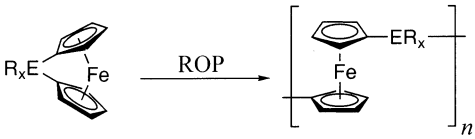

(1)

Results and Discussion

ROP Behavior of the Silicon-Bridged [1]Metallocenophanes 1a and 1b. Our first attempts to obtain a polymer-supported Ziegler−Natta catalyst involved the exposure of **1a** and **1b**[10] to conditions known to induce ROP in strained [1]ferrocenophanes.[9] Although formally analogous to [1]ferrocenophanes, in the zirconocenophane system the cyclopentadienyl ligands are inherently tilted. Much less strain would therefore be expected in **1a** and **1b**. Indeed, these compounds proved to be thermally stable up to 300 °C and were found to decompose rather than polymerize at higher temperatures. Attempts to induce transition-metal ROP using Pt(0) catalysts, even under reflux, were also unsuccessful.

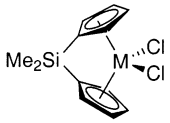

1a (M = Ti)
1b (M = Zr)

In discussing the strain present in metallocenophanes it is helpful to define several angles (Figure 1) including the effective tilt angle (α′), which is the increase in the angle between the planes of the Cp rings relative to an unbridged system, such as (η^5-$MeC_5H_4)_2ZrCl_2$ (**2**) (α = 54.2°)[11] in the case of the zirconium system. Compounds **1a** and **1b** appear to be unstrained; the effective tilt angles are −2.1° and 2.6°, respectively, which are not significantly different from those of unbridged systems.[10] In contrast, ROP of iron-group metallocenophanes requires Cp-ligand tilt angles of greater than 13° relative to the preferred parallel configuration.[9]

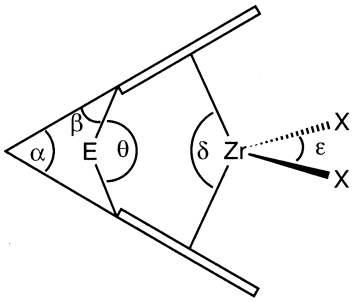

Figure 1. Relationships between *ansa*-zirconocene components defining angle α, α′, *β*, *θ*, *δ*, and *ϵ* (α′ = α − 54.2°).

Scheme 1

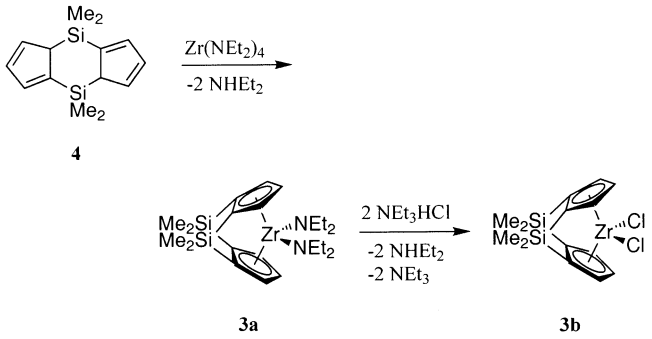

Synthesis of 3a and ROP Behavior of the Doubly Bridged [1][1]Zirconacenophanes 3a and 3b. We have observed in ferrocenophane systems that an increase in tilt angle between the planes of the Cp rings (α) leads to an increase in strain of the molecule and a higher propensity to undergo ROP.[9d] Therefore, we proposed that introduction of a second $SiMe_2$ bridge would further constrain the system and might lead to a polymerizable monomer.

Compound **3a** was synthesized via an amine elimination, in the reaction between the doubly bridged disila-*s*-indacene (**4**) and $Zr(NEt_2)_4$, of the type developed by Jordan and co-workers.[12,13] Subsequent chlorination (Scheme 1) using triethylammonium chloride gave **3b** in high yields (>90%), especially as compared with the previously used method, which involved reaction of the dilithiated ligand system with zirconium tetrachloride.[14]

In the presence of 4 mol % $PtCl_2$, with a sonicating water bath employed to disperse the insoluble catalyst throughout the heterogeneous reaction mixture, no ROP

(7) For recent examples see: (a) Arai, T.; Ban, H. T.; Uozumi, T.; Soga, K. *J. Polym. Sci. A: Polym. Chem.* **1998**, *36*, 421−428. (b) Roscoe, S. B.; Fréchet, J. M. J.; Walzer, J. F.; Dias, A. J. *Science* **1998**, *280*, 270−273. (c) Barrett, A. G. M.; de Miguel, Y. R. *Chem. Commun.* **1998**, 2079−2080.

(8) Recently a significant amount of work has been reported on the placement of organometallic complexes at the periphery of dendrimers. For an example of a dendrimer with a zirconocene complex at the periphery see: Cadierno, V.; Igau, A.; Donnadieu, B.; Caminade, A.-M.; Majoral, J.-P. *Organometallics* **1999**, *18*, 1580−1582.

(9) (a) Foucher, D. A.; Tang, B.-Z.; Manners, I. *J. Am. Chem. Soc.* **1992**, *114*, 6246−6248. (b) Manners, I. *Chem. Commun.* **1999**, 857−865. (c) Manners, I. *Can. J. Chem.* **1998**, *76*, 371−381. (d) Resendes, R.; Nelson, J. M.; Fischer, A.; Jäkle, F.; Bartole, A.; Lough, A. J.; Manners, I. *J. Am. Chem. Soc.* **2001**, *123*, 2116−2126.

(10) Bajgur, C. S.; Tikkanen, W. R.; Petersen, J. L. *Inorg. Chem.* **1985**, *24*, 2539−2546.

(11) Petersen, J. L.; Egan, J. W., Jr. *Inorg. Chem.* **1983**, *22*, 3571−3575. (η^5-$C_5H_5)_2ZrCl_2$ was not chosen as an example for a typical unstrained tilt angle due to the fact that its crystal structure contains two independent molecules in the unit cell which have differing tilt angles and one of which is disordered. See: Prout, K.; Cameron, T. S.; Forder, R. A.; Critchley, S. R.; Denton, B.; Rees, G. V. *Acta Crystallogr.* **1974**, *B30*, 2290−2304.

(12) Diamond, G. M.; Rodewald, S.; Jordan, R. F. *Organometallics* **1995**, *14*, 5−7.

(13) Diamond, G. M.; Jordan, R. F.; Petersen, J. L. *J. Am. Chem. Soc.* **1996**, *118*, 8024−8033.

(14) Cano, A.; Cuenca, T.; Gómez-Sal, P.; Royo, B.; Royo, P. *Organometallics* **1994**, *13*, 1688−1694.

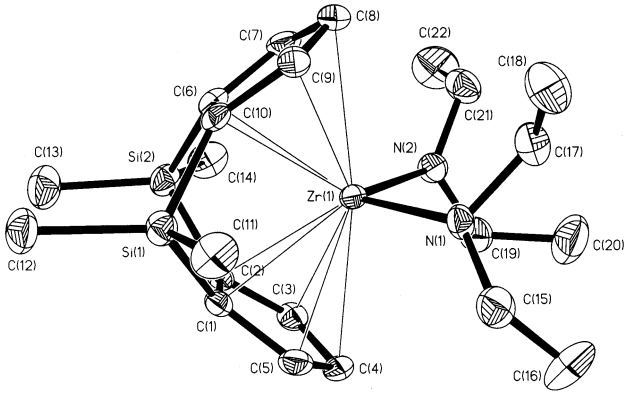

Figure 2. Molecular structure of **3a** showing thermal ellipsoids at 30% probability.

of **3a** was detected by ^{1}H NMR. When the concentration of catalyst was increased to 40 mol %, formation of **3b** as well as the analogous monochlorinated *ansa*-zirconocene $(SiMe_2)_2(\eta^5\text{-}C_5H_3)_2Zr(NEt_2)Cl$ (**3c**) was observed using ^{1}H, ^{13}C, and ^{29}Si NMR spectroscopy. The formation of **3c** was evidenced by the appearance of NMR resonances indicative of a species with lower symmetry: two ^{29}Si resonances indicated the diastereotopic nature of these nuclei, and corresponding loss of the symmetry of the methyl groups and within the Cp rings was evident in the ^{1}H and ^{13}C NMR spectra. To confirm the chlorine exchange with $PtCl_2$, the 1:1 reaction of **3a** with $PtCl_2$ was investigated. Over a 16 h period the initial formation of the monochlorinated species **3c** and its subsequent conversion to the dichlorinated complex **3b** was detected.[15]

All attempts to polymerize **3b** in the presence of catalytic amounts of $PtCl_2$ were unsuccessful. Also, no reaction of **3a** or **3b** was observed in the presence of Karstedt's catalyst. The molecular structure of **3a** was determined by single-crystal X-ray diffraction (Figure 2) and shows an effective tilt angle (α′) of 18.9°, which represents a significant increase in tilt angle relative to the unbridged species (selected data Tables 1−2). The crystal structure of **3b**, as determined by Royo and coworkers,[14] shows an effective tilt angle (α′) of 15.4°, which is also in the range necessary to cause significant strain in ferrocenophanes. The reason for the apparent lack of strain in these systems has recently been clarified by a theoretical study conducted by Green.[16a] Unlike ferrocene derivatives, zirconocene complexes possess a naturally bent structure, and the introduction of a tether between the two cyclopentadienyl ligands does not induce a significant amount of strain in the system, despite an increase in the dihedral angle (α) between the planes of the Cp rings. For a D_{5h} metallocene such as ferrocene the three frontier orbitals, which are primarily metal-d orbital in character, are filled. Upon tilting, the symmetry of a metallocene is reduced from D_{5h} to C_{2v}. In the case of ferrocene an overall increase in energy is observed, largely due to occupation of the HOMO, whose energy rises significantly with tilt angle.[16b] In the case of d^0 zirconocenes there is no occupation of this molecular orbital, and so no corresponding increase in energy is observed upon tilting.[16]

Scheme 2

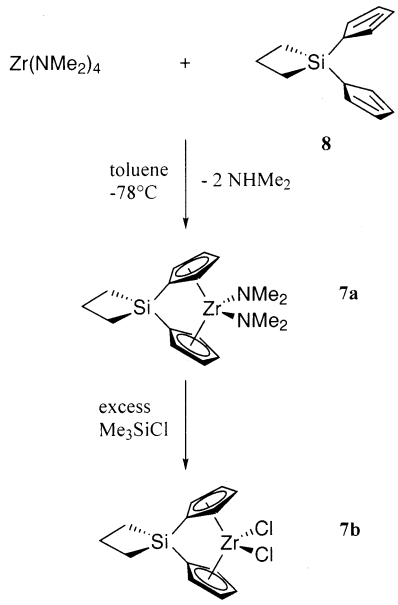

Synthesis and Characterization of 7a and 7b. As an alternative strategy, introduction of a tether which is in itself a strained silacycle should give rise to a monomer that would be polymerizable by ring-opening routes. The system described herein is the silacyclobutane-bridged system.

Silacyclobutanes, such as $(CH_2)_3SiPh_2$ (**5**), have been shown to polymerize both thermally and via transition-metal catalysis to afford polycarbosilanes (e.g., **6**) (eq 2).[17] We envisaged that using the silacyclobutane group as a tether, as in species such as **7a** and **7b**, should allow the zirconocene moiety to remain intact and bound to the polymer backbone by not only one, but both cyclopentadienyl ligands following ROP (eq 3). Unlike many previously reported systems where the active catalytic site is introduced by modification of a previously synthesized polymer, the catalytic center is contained in the monomer, which allows for controlled incorporation of the catalytic moiety into the polymeric system.

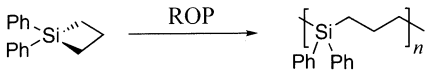

(2)

5 **6**

The synthesis of the monomer **7a** (Scheme 2) was carried out by use of a fly trap process involving the novel cyclotrimethylenedicyclopentadienylsilane (**8**). Com-

(15) No soluble Pt-containing species were isolable from solution. It is likely that an initial metathesis between **3a** and $PtCl_2$ occurs, which gives rise to an unstable Pt-amido compound that decomposes rapidly in solution. The formation of an insoluble black material, presumably Pt metal, was observed over the course of the reaction, and $[NH_2Et_2]Cl$ was isolated from the reaction mixture and identified by ^{1}H NMR. The origin of the hydrogen bound to nitrogen is currently unknown.

(16) (a) Green, J. C. *Chem. Soc. Rev.* **1998**, *27*, 263−271. (b) Barlow, S.; Drewitt, M. J.; Dijkstra, T.; Green, J. C.; O'Hare, D.; Whittingham, C.; Wynn, H. H.; Gates, D.; Manners, I.; Nelson, J. M.; Pudelski, J. K. *Organometallics* **1998**, *17*, 2113−2120.

(17) (a) Ushakov, N. V.; Finkel'shtein, E. Sh.; Babich, E. D. *Polym. Sci., Ser. A* **1995**, *37*, 320−341, and references therein. (b) Babich, E. D. In *Polymeric Materials Encyclopedia*; Salamone, J. C., Ed.; CRC Press: New York, 1996; Vol. 10, pp 7621−7635, and references therein. (c) Cundy, C. S.; Eaborn, C.; Lappert, M. F. *J. Organomet. Chem.* **1972**, *44*, 291−297. (d) Rushkin, I. L.; Interrante, L. V. *Macromolecules* **1996**, *29*, 5784−5787.

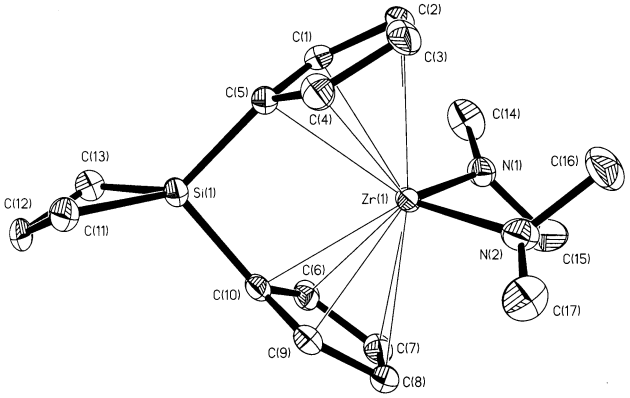

Figure 3. Molecular structure of **7a** showing thermal ellipsoids at 30% probability.

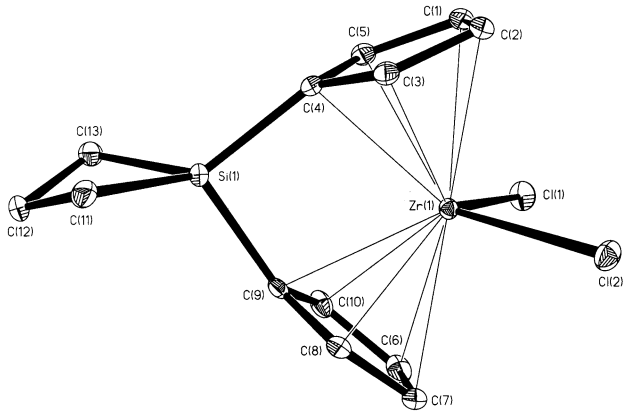

Figure 4. Molecular structure of **7b** showing thermal ellipsoids at 30% probability.

pound **8** was prepared via the reaction of 2 equiv of $Li[C_5H_5]$ with the dichlorosilane $(CH_2)_3SiCl_2$. This species was then reacted, at −78 °C in toluene, with tetrakis(dimethylamido)zirconium to yield **7a** as bright yellow crystals after workup. The substitution of the NMe_2 groups of **7a** for chloro substituents using excess Me_3SiCl was found to be quite facile and gave a high yield (∼51%) of the colorless crystals, **7b**.

^{29}Si, ^{13}C, and ^{1}H NMR spectra for both **7a** and **7b** were consistent with the expected structures. The positions of the two cyclopentadienyl pseudo-triplets in the ^{1}H and ^{13}C NMR are typical for silicon-bridged *ansa*-zirconocenes such as **1b** and $(Et_2Si)(\eta^5\text{-}C_5H_4)_2ZrCl_2$.[10]

Single-crystal X-ray diffraction studies of **7a** and **7b** were undertaken and gave further information on the structure of the compounds. Views of the molecular structures of these species are shown in Figures 3 and 4, respectively. Some key structural features of these compounds are given in Tables 3−6 and are summarized in Table 7, including the angles α, α′, β, θ, δ, and ϵ (defined in Figure 1). The α′ angle for both compounds is similar to that of other mono-bridged zirconocenophanes (e.g., **1b**)[10] that, despite an increase in tilt angle over the unbridged zirconocenophane **2** (α = 54.2°),[11] show no tendency toward ring-opening polymerization (vide supra).

Despite this inherent lack of strain in the zirconacycle, the silacyclobutane moiety is clearly strained. The C−Si−C bond angles of 79.7(2)° and 80.65(10)° for **7a** and **7b**, respectively, are small compared with the tetrahedral angle of 109.5° that would be expected for an unstrained silicon atom. The C−C−C angles (100.8(3)° and 101.1(2)°, respectively) are also significantly smaller than the tetrahedral angle, and the ring puckers defined as the angles between the planes represented by the C(11)−Si(1)−C(13) and C(11)−C(12)−C(13) moieties (21.0(4)° and 22.4(1)°, respectively) are intermediate to those of cyclotrimethylenedimethylsilane (30(2)°)[18] and the ferrocenophane analogue **9** (20.6(2)°),[19] which have both previously been shown to undergo ROP.

Table 1. Selected Bond Lengths (Å) of Compound 3a

type	length	type	length
Zr_1-N_1	2.097(4)	Zr_1-N_2	2.095(4)
Si_1-C_1	1.879(4)	Si_1-C_{10}	1.872(4)
Si_2-C_6	1.870(5)	Si_2-C_{13}	1.874(6)

Table 2. Selected Bond Angles (deg) of Compound 3a

type	angle	type	angle
$N_1-Zr_1-N_2$	98.30(15)	$C_1-Si_1-C_{10}$	93.7(2)
$C_6-Si_2-C_{13}$	117.5(2)		

Table 3. Selected Bond Lengths (Å) of Compound 7a

type	length	type	length
Zr_1-N_1	2.114(3)	Zr_1-N_2	2.099(3)
Si_1-C_5	1.899(3)	Si_1-C_{10}	1.899(3)
Si_1-C_{11}	1.902(3)	Si_1-C_{13}	1.895(4)

Table 4. Selected Bond Angles (deg) of Compound 7a

type	angle	type	angle
$N_1-Zr_1-N_2$	98.56(13)	$C_5-Si_1-C_{10}$	96.52(14)
$C_{11}-Si_1-C_{13}$	79.7(2)		

Table 5. Selected Bond Lengths (Å) of Compound 7b

type	length	type	length
Zr_1-Cl_1	2.4456(7)	Zr_1-Cl_2	2.4305(8)
Si_1-C_4	1.864(2)	Si_1-C_9	1.864(2)
Si_1-C_{11}	1.862(2)	Si_1-C_{13}	1.868(2)

Table 6. Selected Bond Angles (deg) of Compound 7b

type	angle	type	angle
$Cl_1-Zr_1-Cl_2$	100.01(3)	$C_4-Si_1-C_9$	94.68(9)
$C_{11}-Si_1-C_{13}$	80.65(10)		

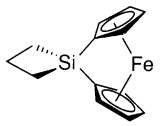

9

ROP Behavior of 7a and 7b. Both **7a** and **7b** were tested for ROP behavior under transition-metal-catalyzed conditions. Attempts to induce the ROP of **7a** using $PtCl_2$ resulted in NMe_2-Cl exchange and no formation of polymer. With Karstedt's catalyst, only

(18) Mastryukov, V. S.; Dorofeeva, O. V.; Vilkov, L. V.; Cyvin, B. N.; Cyvin, S. J. *J. Struct. Chem. (Engl. Trans.)* **1975**, *16*, 438−440.
(19) (a) MacLachlan, M. J.; Lough, A. J.; Geiger, W. E.; Manners, I. *Organometallics* **1998**, *17*, 1873−1883. (b) MacLachlan, M. J.; Ginzburg, M.; Coombs, N.; Coyle, T. W.; Raju, N. P.; Greedan, J. E.; Ozin, G. A.; Manners, I. *Science* **2000**, *287*, 1460−1463.

Table 7. Selected Structural Parameters for 1b, 3a, 3b, 7a, and 7b with ESDs in Parentheses

feature	2	1b	3a	3b	7a	7b
Zr−Si (Å)		3.3493(4)	3.286(4)	3.233(3)	3.445(4)	3.330(4)
Zr−X av (Å)	2.443(1)	2.435(1)	2.096(4)	2.428(1)	2.106(3)	2.4380(8)
Zr−midpoint (Å)	0.952(2)	1.007(4)	1.217(4)	1.090	1.108(4)	0.998(4)
Si−$C_{ipso-Cp}$ av (Å)		1.866(4)	1.874(4)	1.884	1.899(3)	1.864(2)
α (deg)	54.2	56.8	73.1(4)	69.6(1)	61.7(2)	59.69(7)
α′ (deg)	0	2.6	18.9(4)	15.4(1)	7.5(2)	5.49(7)
β av (deg)		17.2	19.7(3)	19.6	18.2(2)	18.2(2)
θ (deg)		93.2(2)	93.3(2)	91.5	96.52(14)	94.68(9)
δ (deg)	128.9(2)	125.4(3)	116.0(3)	120.6(3)	123.0(2)	126.2(2)
ϵ (deg)	95.10(5)	97.98(4)	98.30(15)	99.64(4)	98.56(13)	100.01(3)
ref	11	10	this work	14	this work	this work

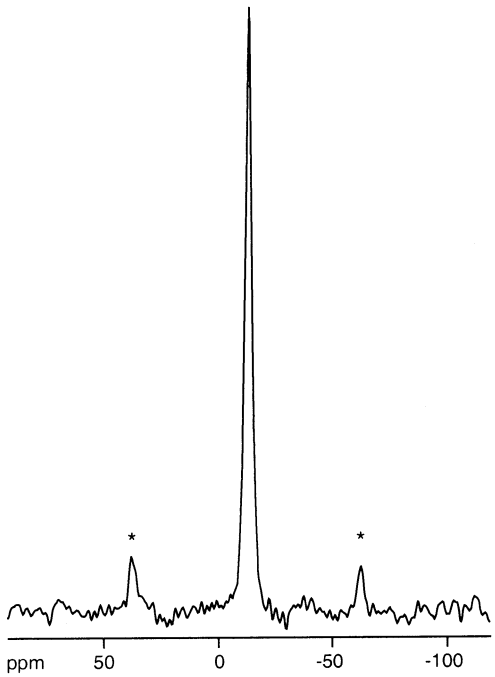

Figure 5. CP-MAS ^{29}Si NMR spectrum of the insoluble fraction of **10** (note spinning sideband peaks (*) for MAS = 4 kHz).

unreacted **7a** was observed in the ^{1}H NMR spectrum of the reaction mixture. However, with ∼3 wt % of Karstedt's catalyst, **7b** was found to undergo ROP in solution at room temperature. Increasing the temperature to ∼55 °C accelerated the reaction from 1 week to 3 days, as observed by ^{1}H NMR. The resultant off-white solid product consisted of soluble (∼30%) and insoluble fractions (∼22%) with a total isolated yield of 52%.

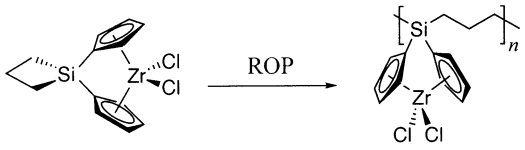

7b **10** (3)

Both fractions were characterized by solid-state CP-MAS ^{29}Si and ^{13}C NMR along with a ^{13}C NMR NQS experiment and showed spectra consistent with the structure of the desired product. The insoluble fraction of **10** showed a single Si environment with a peak at −12.1 ppm (Figure 5). The corresponding ^{13}C NMR spectrum (Figure 6) showed peaks corresponding to the

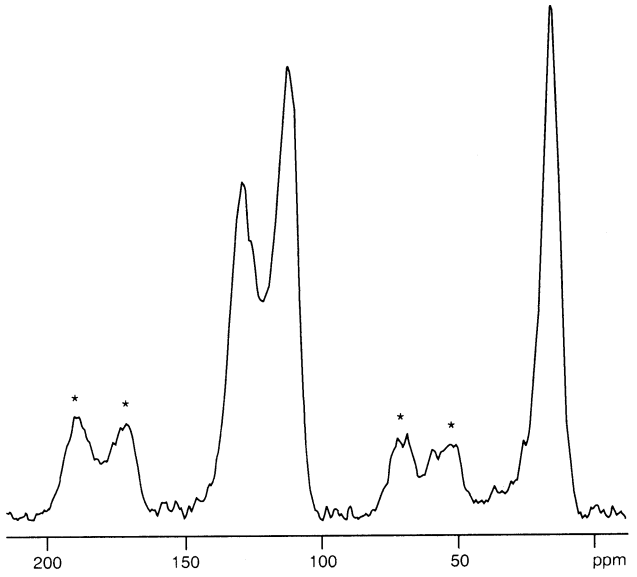

Figure 6. CP-MAS ^{13}C NMR spectrum of the insoluble fraction of **10** (note spinning sideband peaks (*) for MAS = 6 kHz)

Cp environments (130 and 113 ppm) as well as a broad peak corresponding to the methylene moieties in the backbone (17 ppm). The NQS experiment showed the *ipso*-Cp peak to be present at 110 ppm, under the other peaks in the Cp region.

The soluble fraction of the polymer showed very similar solid state CP-MAS spectra with the addition of a side peak in the ^{29}Si NMR at −21.4 ppm and an additional peak in the ^{13}C NMR at 75 ppm that could potentially be due to the end groups. The solution NMR spectra of the soluble fraction were similar to those in the solid state but with the expected slight shifts due to solvent effects. In the solution ^{29}Si NMR spectrum the major peak is found at −13.9 and the minor peak at −22.4 ppm. Interestingly, each peak appeared to consist of a closely spaced cluster of resonances, which is suggestive of the presence of slightly different silicon environments; this would be expected if the material is of low molecular weight. The solution state ^{13}C NMR was less well resolved but showed the Cp peaks at 129.2 and 115.2 ppm as well as the *ipso*-Cp peak at 108.1 ppm as distinct carbon environments. The methylene region was fairly complex with a series of peaks between 18.6 and 12.6 ppm that are consistent with the broad peak in the solid state at 18 ppm. The peak at ∼75 ppm was present but was very weak and is tentatively assigned to an end group. The ^{1}H NMR showed broad Cp proton resonances near those of the monomer, and the methylene proton region between ∼2.3 and ∼0.9 ppm again

Table 8. Comparison of the ^{29}Si NMR Data Obtained from the Transition-Metal-Catalyzed Polymerizations of 7b and 5

	zirconocene-containing		model system	
	$\delta(^{29}Si)$	compd	$\delta(^{29}Si)$	compd
monomer	−0.4[a]	**7b**	8.6[b]	**5**
polymer				
(soluble fract, solution)	−12.5[b]	**10**	−7.7[a]	**6**
(soluble fract., solid)	−13.9		−8.0	
(insoluble fract., solid)	−12.1			

[a] In chloroform-*d*. [b] In dichloromethane-d_2.

Table 9. Solution Semibatch Reactor (SBR) Screening Experiment Data for 7a, 7b, 10, and Some Typical Zirconocene Compounds

catalyst[a]	activity (g PE/mmol Zr h)
7a[b]	1370.64
7b[b]	1829.71
10[c]	340.9
Cp_2ZrCl_2	1339.94
$(Et\text{-}ind)_2ZrMe_2$ [d]	5229.34

[a] SBR standard PMAO-IP screening conditions unless otherwise indicated. [b] 65 and then 325 μmol/L of catalyst. [c] 200 μmol/L of catalyst. [d] Trityl borate screening conditions: B/Zr = 1.05 and PMAO-IP of 1 mmol/L as a scavenger (Et-ind = ethylindenyl).

showed a complex series of peaks suggestive of the chain length effects characteristic of an oligomeric material.

Pyrolysis mass spectrometry was also performed on both the soluble and insoluble fractions of **10**. The two spectra were very similar and showed clear evidence for dimeric fragments, varying only in the intensities of the observed peaks. The observed fragmentation pattern was complex, but peaks providing evidence for cleavage at Zr−(C_5H_4), Si−(C_5H_4), Si−CH_2, and CH_2−CH_2 bonds were observed.

Due to moisture sensitivity of **10** molecular weight estimation by gel permeation chromatography was not possible. Dynamic light scattering (DLS) measurements of the soluble fraction of **10** were carried out and showed that the hydrodynamic radius (R_h) for the soluble fraction was <1 nm. This indicated that this fraction was oligomeric, with a molecular weight (M_w) of < ca. 3000 relative to polystyrene.

To provide further evidence for the formation of the targeted polymeric product, we compared the ^{29}Si NMR spectra of the monomer **7b** and polymer **10** with those of a model silacyclobutane system, $(CH_2)_3SiPh_2$ (**5**), and its ring-opened polymer **6** (Table 8). Although the monomers **7b** and **5** possess fairly different ^{29}Si NMR chemical shifts at −0.4 and 8.6 ppm, respectively, ROP induces similar upfield shifts in each due to changes in the silicon environment. Thus, polymer **10** shows a shift to ca. −13 ppm ($\Delta\delta$ = −12.6 ppm) while the polymer **6** shows a similar upfield shift to ca. −8 ppm ($\Delta\delta$ = −16.6 ppm).

Ethylene Polymerizations. Both of the silacyclobutane-tethered compounds (**7a** and **7b**) underwent preliminary testing for catalytic activity. Under standard solution phase conditions both showed activities comparable to those found for zirconocene dichloride itself and slightly lower than those found for the more active $(Et\text{-}ind)_2ZrMe_2$ (Et-ind = ethylindenyl) (Table 9). Gas phase testing (BSR) was not nearly as promising, showing much lower activities for **7a** and **7b** than for a typical commercial zirconocene catalyst, $(n\text{-}BuCp)_2ZrCl_2$ (Table 10). In both cases the chlorinated monomer **7b** was more active than the dimethylamido-substituted analogue **7a**. Catalytic activity testing on the insoluble fraction of polymer **10** showed fairly low activities in both the solution and gas phase. One possible explanation for this involves the ease of bimolecular deactivation due to proximity of catalytic sites within the polymer. Synthesis of polymers with lower loadings of catalytic sites, through copolymerization strategies, could lead to more active materials in which the catalytic sites are isolated from one another within the polymer matrix. Further work in this area will be undertaken to investigate this possibility.

Table 10. Bench Scale Reactor (BSR) Screening Experiment Data for 7a, 7b, 10, and a Typical Zirconocene Compound

catalyst[a]	activity (g PE/mmol Zr [C_2H_4] h)
7a	653
7b	4837
10[b]	1109
$(n\text{-}BuCp)_2ZrCl_2$	112 272

[a] Standard BSR conditions unless otherwise specified. [b] 58 mg of supported catalyst.

Experimental Section

General Comments. Unless otherwise noted, all chemicals were purchased from Aldrich. Cyclotrimethylenedichlorosilane was purchased from Gelest Inc. Zirconium tetrakis(dimethylamide),[13] zirconium tetrakis(diethylamide),[20,21] **4**,[22] **1a**,[10] and **1b**[23] were synthesized according to literature procedures. Solvents were dried by standard methods, distilled, and stored under nitrogen. For the solution semibatch reactor (SBR) ethylene polymerizations ethylene (99.5%, polymer grade, Matheson) was purified by passage through the SBR gas purification units (13X, COS, Oxiclear), cyclohexane was purified by passage through the SBR solvent purification units (13X, 13A, COS), and PMAO-IP was purchased from Akzo-Nobel and contained 12.9 wt % of Al. The bench scale reactor (BSR) polymerizations used similar purification systems for ethylene, nitrogen, and *n*-hexane, and the Witco MAO SiO_2 used contained 25 wt % of Al.

All manipulations involving air- and moisture-sensitive compounds were performed under an atmosphere of prepurified nitrogen using standard Schlenk techniques or in an inert-atmosphere glovebox. All solution ^{1}H, ^{13}C, and ^{29}Si NMR were recorded on Varian Gemini 300 or Unity 400 spectrometers. ^{29}Si NMR were recorded using either a normal or a DEPT pulse sequence and were referenced externally to TMS. Solid state ^{29}Si CP-MAS NMR spectra were obtained on a Bruker DSX400 spectrometer using a spinning rate of 4 kHz, a recycle delay of 5 s, and a contact time of 5 ms. Solid state ^{13}C NMR spectra were obtained on a Bruker DSX400 spectrometer using a spinning rate of 6 kHz, a recycle delay of 5 s, and a contact time of 2 ms.

Mass spectra were obtained with a Micromass 70-250S mass spectrometer operating in electron impact (EI) mode. GC−MS analysis was carried out with a Hewlett-Packard 5890 Series II gas chromatograph fitted with a Supelco PTE-5 column (30 M × 0.25 mm, 0.25 μm film) and equipped with a Hewlett-Packard 5971 Series mass selective detector.

(20) Bradley, D. C.; Thomas, I. M. *J. Chem. Soc.* **1960**, 3857−3861.
(21) Diamond, G. M.; Jordan, R., F.; Petersen, J. L. *Organometallics* **1996**, *15*, 4030−4037.
(22) Hiermeier, J.; Köhler, F. H.; Müller, G. *Organometallics* **1991**, *10*, 1787−1793.
(23) Yasuda, H.; Nagasuna, K.; Akita, M.; Lee, K.; Nakamura, A. *Organometallics* **1984**, *3*, 1470−1478.

Attempted ROP of 1a and 1b. 1a (0.88 g, 2.9 mmol) or **1b** (1.00 g, 2.9 mmol) was dissolved in toluene (~50 mL). A catalytic amount of $PtCl_2$ (0.008 g, 0.029 mmol, 1 mol %) or Karstedt's catalyst in xylenes (1 mL, ~3 wt %) was added to the solution, and it was allowed to stir overnight. ^{1}H NMR monitoring of an aliquot showed no reaction. The solution was refluxed for a further 24 h with no discernible change in the spectrum.

Synthesis of the [1][1]Zirconocenophane 3a. $Zr(NEt_2)_4$ (4.00 g, 10.6 mmol) and **4** (2.55 g, 10.6 mmol) were combined in a flask fitted with a reflux condenser. To these solids was added 50 mL of toluene. The solution was refluxed overnight, during which time the solution underwent a change in color from light orange to dark red. The solvent was removed under high vacuum and the product recrystallized from hexanes at −30 °C to give pale yellow-orange crystals (yield 4.65 g, 92%): ^{29}Si NMR (79.3 MHz, C_6D_6) δ −18.5 ppm; ^{13}C NMR (75.4 MHz, C_6D_6) δ 130.6 (Cp), 116.7 (*ipso*-Cp), 110.1 (Cp), 50.2 (NCH_2CH_3), 15.2 (NCH_2CH_3), 2.5 ($SiMe_2$), −3.9 ($SiMe_2$) ppm; ^{1}H NMR (300 MHz, C_6D_6) δ 6.73 (d, 4H, Cp), 6.01 (tr, 2H, Cp), 3.28 (q, 8H, NCH_2CH_3), 1.04 (tr, 12H, NCH_2CH_3), 0.72 (s, 6H, $SiMe_2$), 0.41 (s, 6H, $SiMe_2$) ppm. DSC: mp = 130 °C; T_{dec} = 225 °C. Elemental analysis was repeatedly attempted but consistently gave low C and N values. This may be due to the formation of a noncombustible ceramic residue. High-resolution MS for $C_{22}H_{38}N_2Si_2Zr$: calcd 476.162656; found 476.162064. For further evidence of purity see ^{1}H and ^{13}C NMR spectra in Supporting Information.

Synthesis of the [1][1]Zirconacenophane 3b. A solution of NEt_3HCl (0.86 g, 6.30 mmol) in 10 mL of CH_2Cl_2 was added to a stirred solution of **3a** (1.50 g, 3.15 mmol) in 50 mL of CH_2Cl_2 at 0 °C. The reaction mixture was allowed to warm to room temperature overnight. The solution was concentrated and the product recrystallized at −30 °C. The ^{1}H NMR spectrum of the white crystalline product was consistent with literature values[14] (yield 1.16 g, 91%).

Attempted Polymerization of 3a with 4 mol % $PtCl_2$. Compound **3a** (0.250 g, 0.53 mmol) was dissolved in ~0.5 mL of C_6D_6 in a 5 mm NMR tube. A catalytic amount of $PtCl_2$ (0.004 g, 0.02 mmol) was added to this solution, and the NMR tube was then placed in a sonicating water bath and sonicated for 16 h. ^{1}H NMR spectra were run approximately every 4 h, but no resonances other than those due to **3a** were discernible.

Attempted Polymerization of 3a with 40 mol % $PtCl_2$. Compound **3a** (0.250 g, 0.53 mmol) was dissolved in ~0.5 mL of C_6D_6 in a 5 mm NMR tube. $PtCl_2$ (0.04 g, 0.2 mmol) was added to this solution, and the NMR tube was then placed in a sonicating water bath and sonicated for 16 h. ^{1}H NMR spectra were run approximately every 4 h. In addition to the resonances due to **3a** new resonances in the cyclopentadienyl, ethylamido, and methyl regions were observed and increased in intensity over the course of the study. The number of resonances indicated two new products, one of which was consistent with **3b**. The second product was determined to be the analogous monochlorinated species **3c**. The ^{29}Si, ^{13}C, and ^{1}H NMR spectra for this species were determined from the spectra of the mixture by process of elimination. For **3c**: ^{29}Si NMR (79.3 MHz, C_6D_6) δ −17.1 (s, $SiMe_2$), −18.5 (s, $SiMe_2$) ppm; ^{13}C NMR (100 MHz, C_6D_6) δ 138.7 (Cp), 130.5 (Cp), 125.6 (*ipso*-Cp), 113.8, (*ipso*-Cp), 112.1 (Cp), 51.2 (NCH_2CH_3), 14.7 (NCH_2CH_3), 2.2 ($SiMe_2$), 1.4($SiMe_2$), −4.0 ($SiMe_2$), −4.5 ($SiMe_2$) ppm; ^{1}H NMR (400 MHz, C_6D_6) δ 6.87 (m, 2H, Cp), 6.46 (m, 2H, Cp), 6.02 (m, 2H, Cp), 3.38 (q, 4H, NCH_2CH_3), 0.96 (tr, 6H, NCH_2CH_3), 0.60 (s, 3H, $SiMe_2$), 0.54 (s, 3H, $SiMe_2$), 0.26 (s, 3H, $SiMe_2$), 0.22 (s. 3H, $SiMe_2$) ppm.

1:1 Reaction of 3a with $PtCl_2$. Compound **3a** (0.050 g, 0.11 mmol) was dissolved in ~0.5 mL of C_6D_6 in a 5 mm NMR tube. $PtCl_2$ (0.028 g, 0.11 mmol) was added to this solution, and the NMR tube was then placed in a sonicating water bath and sonicated for 16 h. ^{1}H NMR spectra were run approximately every 4 h. Resonances due to **3b** were observed to increase in intensity in the ^{1}H NMR spectrum over this time until there was no evidence for **3a** or the monochlorinated species **3c**. A white precipitate was found at the bottom of the NMR tube. This precipitate was isolated by filtration under an inert N_2 atmosphere, characterized by ^{1}H NMR, and identified as NEt_2H_2Cl: ^{1}H (400 MHz, $CDCl_3$) δ 9.48 (br, 2H, NH_2), 3.10 (q, 4H, NCH_2), 1.52 (tr, 6H, CH_3) ppm.

Attempted Pt-Catalyzed ROP of 3b. Compound **3b** (1.00 g, 2.5 mmol) was dissolved in toluene (~50 mL). A catalytic amount of $PtCl_2$ (0.007 g, 0.026 mmol, 1 mol %) or Karstedt's catalyst in xylenes (1 mL, ~3 wt %) was added to the solution, and it was allowed to stir overnight. ^{1}H NMR monitoring showed no reaction. The solution was refluxed for a further 24 h with no discernible change in the spectrum.

Preparation of Cyclotrimethylenedicyclopentadienylsilane 8. A solution of LiCp (15.72 g, 218.4 mmol) in THF (~300 mL) was added dropwise via cannula over 1 h to a stirred solution of cyclotrimethylenedichlorosilane (14.00 g, 99.3 mmol) in THF (~100 mL) at − 78 °C. The reaction mixture was allowed to stir while warming up to room temperature, and the solvent was subsequently removed under vacuum. The product was taken up in hexanes (~350 mL), filtered through Celite to give a clear, faint yellow solution, and placed in a freezer at −50 °C overnight. The solution was gravity filtered to remove any orange solid, and the hexanes were removed under reduced pressure to yield a viscous yellow liquid (15.62 g, 79%). Compound **8** was stored under nitrogen at −40 °C and used without further purification. The product was characterized using ^{29}Si, ^{1}H NMR, and GC−MS: ^{29}Si NMR (79.3 MHz, C_6D_6, 298 K) δ 14.6 ppm; ^{1}H NMR (400 MHz, C_6D_6, 298 K) δ 6.8−6.0 (br, 10H, Cp), 1.86 (quintet, 2H, CH_2), 0.82 (tr, 4H, Si-CH_2) ppm; GC−MS 200 (10, M^+), 135 (100, M^+ − Cp).

Synthesis of 7a. A solution of **8** (6.06 g, 30.3 mmol) in toluene (~150 mL) was added dropwise via cannula over 1 h to a solution of $Zr(NMe_2)_4$ (8.09 g, 30.3 mmol) in toluene (~150 mL) at −78 °C. The mixture was allowed to warm to room temperature overnight, and the solvent was removed under vacuum to yield crude **7a**. Purified **7a** was obtained by sublimation (80 °C, 5×10^{-3} mmHg) in reasonable yields (6.35 g. 56%) as a bright yellow crystalline material: ^{29}Si NMR (79.3 MHz, C_6D_6) δ −0.99 ppm; ^{13}C NMR (100 MHz, C_6D_6) δ 117.3 (Cp), 112.2 (*ipso*-Cp), 109.7 (Cp), 48.8 (NMe_2), 18.6 (CH_2), 13.9 ($SiCH_2$) ppm; ^{1}H NMR (400 MHz, C_6D_6) δ 6.53 (m, 4H, Cp), 5.71 (m, 4H, Cp), 2.75 (s, 12H, NMe_2), 2.27 (quintet, $^3J_{HH}$ = 8.4 Hz, 2H, CH_2), 1.49 (tr, $^3J_{HH}$ = 8.4 Hz, 4H, $SiCH_2$), ppm; MS (EI, 70 eV) 376 (26, M^+), 330 (100, $M^+ - N(CH_3)_2$, $-H_2$). Elemental analysis was repeatedly attempted but consistently gave low C and N values. This may be due to the formation of a noncombustible ceramic residue. High-resolution MS for $C_{17}H_{26}N_2SiZr$: calcd 376.090606; found 376.091235. For further evidence of purity see ^{1}H and ^{13}C NMR spectra in Supporting Information.

Synthesis of 7b. A solution of **7a**, prepared by the reaction of **8** (6.91 g, 34.6 mmol) and $Zr(NMe_2)_4$ (9.07 g, 34.0 mmol), was reacted in situ with an excess of chlorotrimethylsilane (~13 mL, 102 mmol, 3 equiv). **7b** was isolated as colorless crystals after recrystallization from CH_2Cl_2/hexanes (6.22 g, 51%): ^{29}Si NMR (79.3 MHz, $CDCl_3$) δ −0.36 ppm; ^{13}C NMR (100 MHz, $CDCl_3$) δ 128.3 (Cp), 113.8 (Cp), 108.4 (*ipso*-Cp), 18.25 (CH_2), 14.03 ($SiCH_2$) ppm; ^{1}H NMR (400 MHz, $CDCl_3$) δ 6.98 (m, 4H, Cp), 6.03 (m, 4H, Cp), 2.47 (quintet, $^3J_{HH}$ = 8.4 Hz, 2H, CH_2), 1.72 (tr, $^3J_{HH}$ = 8.4 Hz, 4H, $SiCH_2$) ppm; MS (EI, 70 eV) 360 (45, M^+), 322 (100, M^+ − HCl, $-H_2$). Anal. Calcd for $C_{13}H_{14}Cl_2SiZr$: C 43.32, H 3.91. Found: C 42.76, H 3.85.

Transition-Metal-Catalyzed ROP of 7b; Synthesis of 10. A catalytic amount of Karstedt's catalyst in xylenes (0.7 mL, ~3 wt %) was added to a solution of **7b** (0.638 g, 1.77 mmol) in THF at 25 °C. The solution was heated to 55 °C and monitored daily by ^{1}H NMR spectroscopy. After 3 days there

Table 11. Summary of Crystallographic Data

	3a	7a	7b
empirical formula	$C_{22}H_{38}N_2Si_2Zr$	$C_{17}H_{26}N_2SiZr$	$C_{13}H_{14}Cl_2SiZr$
fw	477.94	377.71	360.45
	yellow-orange crystals	yellow crystals	colorless crystals
tenperature (K)	243(2)	223(2)	130(1)
wavelength (Å)	0.71073	0.71073	0.71073
cryst syst, space group	monoclinic, $P2_1/c$	triclinic, $P\bar{1}$	triclinic, $P\bar{1}$
unit cell dimens			
a (Å)	8.0131(8)	8.2103(2)	7.3911(15)
b (Å)	9.2651(8)	8.53240(10)	8.7010(17)
c (Å)	32.692(5)	14.7223(3)	10.800(2)
α (deg)	90	94.6170(10)	86.89(3)
β (deg)	94.950(10)	99.0970(10)	82.13(3)
γ (deg)	90	113.1860(10)	88.32(3)
volume (Å^3)	2418.1(5)	924.48(3)	686.8(2)
Z	4	2	2
D_{calcd} (g cm^{-3})	1.313	1.357	1.743
abs coeff (mm^{-1})	0.563	0.656	1.250
F(000)	1008	392	360
cryst size (mm)	0.40 × 0.30 × 0.20	0.40 × 0.40 × 0.15	0.25 × 0.20 × 0.10
θ range for data collection (deg)	$2.29 < \theta < 21.49$	$1.42 < \theta < 27.92$	$2.78 < \theta < 26.37$
limiting indices	$-1 \le h \le 8$,	$-10 \le h \le 9$,	$0 \le h \le 9$,
	$-1 \le k \le 9$,	$-10 \le k \le 9$,	$-10 \le k \le 10$,
	$-33 \le l \le 33$	$-19 \le l \le 18$	$-13 \le l \le 13$
no. of reflns collected	4057	6107	6885
no. of ind reflns	2781 (R_{int} = 0.0401)	3834 (R_{int} = 0.0221)	2778 (R_{int} = 0.024)
no. of data/restraints/params	2780/0/245	3813/0/190	2778/0/155
goodness of fit on F^2	1.269	1.082	1.072
final R indices [$I>2\sigma(I)$]	R1 = 0.0390,	R1 = 0.0359,	R1 = 0.0229,
	wR2 = 0.0870	wR2 = 0.1226	wR2 = 0.0604
R indices (all data)	R1 = 0.0486,	R1 = 0.0460,	R1 = 0.0256,
	wR2 = 0.0893	wR2 = 0.1776	wR2 = 0.0611
extinction coeff	0.0077(5)		0.0182(17)
largest diff peak and hole (e Å^{-3})	0.378 and −0.428	0.747 and −0.845	0.418 and −0.674

was no more evidence for monomer and the insoluble off-white solid was removed by filtration (0.140 g, 22%). The soluble fraction was precipitated into dry hexanes and isolated by filtration as an off-white, air-sensitive solid (0.190 g, 30%). The soluble fraction was found to be soluble in THF, DMSO, and CH_2Cl_2, but not in $CHCl_3$, Et_2O, or hexanes, while the insoluble fraction did not dissolve in any of these.

Insoluble fraction: CP-MAS ^{29}Si NMR (79.49 MHz, 4 kHz) δ −12.1 ppm; CP-MAS ^{13}C NMR (100.6 MHz, 6 kHz) δ 130 (Cp), 113 (Cp), 17 (methylene) ppm; NQS ^{13}C NMR (100.6 MHz, d3 = 1 ms) δ 110 ppm; pyrolysis MS (EI, 70 eV) 719 (11, $M_2^+ - H$), 693 (7, $M_2^+ - C_2H_4 + H$), 399 (24, $M_2^+ - (C_5H_4)_2ZrCl_2 - C_2H_4 - H_2 - H$), 358 (27, $M^+ - H_2$), 346 (25, $(C_5H_4)_2ZrCl_2Si(CH_2)_2^+$), 332 (31, $(C_5H_4)_2ZrCl_2SiCH_2^+$), 318 (23, $(C_5H_4)_2ZrCl_2Si^+$), 289 (26, $(C_5H_4)_2ZrCl_2^+ - H$), 224 (100, $C_5H_4ZrCl_2^+$), 163 (18, $ZrCl_2^+ + H$). Anal. Calcd for insoluble fraction $C_{13}H_{14}Cl_2SiZr$: C 43.32, H 3.91. Found: C 42.63, H 3.79.

Soluble fraction: CP-MAS ^{29}Si NMR (79.49 MHz, 4 kHz) δ −12.5, −21.4 ppm; CP-MAS ^{13}C NMR (100.6 MHz, 6 kHz) δ 130 (Cp), 115 (Cp), 75, 18 (methylene) ppm; NQS ^{13}C NMR (100.6 MHz, d3 = 1 ms) δ 109 ppm; ^{29}Si NMR (79.3 MHz, CD_2Cl_2) δ −13.9, −22.4 ppm; ^{13}C NMR (100.4 MHz, CD_2Cl_2) δ 129.2 (Cp), 115.2 (Cp), 108.1 (*ipso*-Cp), 75, 18.6−12.6 (−CH_2−) ppm; ^{1}H NMR (399.3 MHz, CD_2Cl_2) δ 6.94 (Cp), 6.49, 6.03 (Cp), 5.81, 2.89, 2.04 (CH_2), 1.94 (CH_2), 1.67 (CH_2), 1.55 (CH_2), 1.40 (CH_2), 1.29 (CH_2), 1.12 (CH_2), 0.97 (CH_2), 0.88 (CH_2) ppm; pyrolysis MS (EI, 70 eV) 719 (5, $M_2^+ - H$), 693 (3, $M_2^+ - C_2H_4 + H$), 399 (11, $M_2^+ - (C_5H_4)_2ZrCl_2 - C_2H_4 - H_2 - H$), 358 (11, $M^+ - H_2$), 346 (10, $(C_5H_4)_2ZrCl_2Si(CH_2)_2^+$), 332 (3, $(C_5H_4)_2ZrCl_2SiCH_2^+$), 317 (13, $(C_5H_4)_2ZrCl_2Si^+ - H$), 289 (36, $(C_5H_4)_2ZrCl_2^+ - H$), 224 (100, $C_5H_4ZrCl_2^+$), 163 (16, $ZrCl_2^+ + H$). Dynamic light scattering measurements indicated that the hydrodynamic radius (R_h) of the soluble fraction in THF was under the lower detection limit of 1 nm. This indicates a molecular weight (M_w) of < ca. 3000.

X-ray Crystallography. X-ray crystallographic data (Table 11) were collected on Siemens P4 diffractometers with smart CCD detectors using graphite-monochromated Mo Kα radiation (λ = 0.71073 Å). The structures were solved and refined using the SHELXTL\PC V5.1 package.[24]

For **3a**: The data frames were integrated and scaled using the Bruker routines SAINT and SADABS. Refinement was by full-matrix least-squares on F^2 using all data (negative intensities included) except for one with very negative F^2 or flagged by the user for potential systematic errors. The weighing scheme was $w = 1/[\sigma^2(F_o^2) + (0.0300P)^2 + 0.0000P]$ where $P = (F_o^2 + 2F_c^2)/3$. Hydrogen atoms were included in calculated positions.

For **7a**: The data frames were integrated and scaled using the Bruker routines SAINT and SADABS. Refinement was by full-matrix least-squares on F^2 using all data (negative intensities included) except for 21 with very negative F^2 or flagged by the user for potential systemtic errors. The weighing scheme was $w = 1/[\sigma^2(F_o^2) + (0.1000P)^2 + 0.0000P]$ where $P = (F_o^2 + 2F_c^2)/3$. Hydrogen atoms were included in calculated positions.

For **7b**: 180 frames of 1° rotations of ϕ and ω (with κ offsets) were exposed for 90 s each. The data frames were integrated and scaled using the Denzo-SMN package.[25] Refinement was by full-matrix least-squares on F^2 using all data (negative intensities included). The weighing scheme was $w = 1/[\sigma^2(F_o^2) + (0.0081P)^2 + 0.1465P]$ where $P = (F_o^2 + 2F_c^2)/3$. Hydrogen atoms were included in calculated positions.

Ethylene Polymerizations. Solution semibatch reactor (SBR) screening experiments were carried out (solution phase). The SBR uses a programmable logic control system with Wonderware 5.1 software for process control. The ethylene polymerizations were performed in a 500 mL Autoclave Engineers Zipperclave reactor equipped with an air-driven stirrer and an automatic temperature control system. All chemicals were fed into the reaction batchwise except ethylene,

(24) Sheldrick, G. M. In *SHELXTL\PC* v5.1 ed.; Bruker Analytical X-Ray Systems: Madison, WI, 1997.
(25) Otwinowski, Z.; Minor, W. *Methods Enzymol.* **1997**, *276*, 307−326.

which was fed on demand. All experiments were carried out under standard SBR conditions (as follows): ~220 mL of cyclohexane, 65−325 μmol/L catalyst, Al/Zr = 300:1 for the PMAO-IP cocatalyst, 160 °C, 140 psig total (0.75 wt % of ethylene in the liquid phase), and a stirring speed of 2000 rpm. The polymerization time was 10 min in each case. The reaction was terminated by addition of 5 mL of methanol, and polymer was recovered by evaporation of the cyclohexane.

Prior to carrying out research on the SBR the stirring speed effect on the mass transfer of ethylene from gas to liquid phase (based on the ethylene consumption of a relatively active catalyst $(Et\text{-}ind)_2ZrCl_2$ + MMAO-3) was investigated. No mass transfer limitation was found when the stirring speed was ≥2000 rpm.

The temperature control unit of the SBR is composed of two components, a manual control of the furnace temperature and an automatic control of the cooling water. Before a polymerization reaction occurred, the reactor temperature oscillated around the set point of 160 °C (155.5−162 °C). For standard run conditions with $(Et\text{-}ind)_2ZrCl_2$ + MMAO-3, the reaction temperature initially overshot to 169 °C in the first 30 s, then returned to the set point temperature of 160 °C within a minute. This effect applies to most catalysts tested on the SBR under the standard conditions.

Bench scale reactor (BSR) experiments were also carried out (gas phase). The system design includes a 2 L semibatch stirred steel reactor with ethylene and comonomer (1-butene) feed on demand, catalyst supply at the beginning, and no product discharge. All experiments were carried out under standard BSR conditions (as follows): 160 g of NaCl, 10−50 mg of catalyst (0.1 mmol[M]/g), Witco MAO SiO_2 with 25 wt % of Al, 90 °C, 200 psig total, a comonomer 1-butene concentration of 0−4%, and a stirring speed of 1800 rpm. The polymerization time was 1 h in each case, and the reaction was terminated by venting the reactor.

Acknowledgment. T.J.P. would like to thank NSERC for a graduate scholarship, P.N. would like to thank NSERC for a post-doctoral fellowship, and S.C.B. would like to thank the University of Toronto and the Ontario Government for graduate scholarships, respectively. I.M. would like to thank the Ontario government for a PREA Award, and NSERC and Nova Chemicals for funding the research.

Supporting Information Available: Crystallographic tables of bond lengths, bond angles, and atomic coordinates for **3a**, **7a**, and **7b** and ^1H and ^{13}C NMR spectra for **3a** and **7a**. This material is available free of charge via the Internet at http://pubs.acs.org.

OM001023P